

Characterisation of nanopipettes for nanoparticles experiments

Author: Júlia Cano Canals

Facultat de Física, Universitat de Barcelona, Diagonal 645, 08028 Barcelona, Spain.

Advisors: Alejandro Colchero Truniger and Félix Ritort Farrán

(Dated: June 16, 2022)

Abstract: The purpose of this work has been to produce quartz nanopipettes with a diameter at the tip of about 200 – 300 nm using a Laser-Based Micropipette Puller. The nanopipettes have been characterized using optical and electronic imaging, and by measuring their conductance in a salt solution. We have come up with a formula relating the conductance and geometry of the nanopipettes. This formula can be used to estimate the size of the nanopipette aperture at the tip from its conductance. This is helpful for approximating the aperture without having to use a scanning electron microscope (SEM). Finally we have tested the nanopipettes by performing translocations of mesoporous silica nanoparticles (NPs) using the resistive pulse sensing technique.

I. INTRODUCTION

Nanoparticles (NPs) have lately received much scientific attention due to their wide range of application. To detect NPs and study their properties, one can use the resistive-pulse sensing method based on the Coulter principle [1]. In this technique, two reservoirs filled with a salt solution are connected with a nanopipette. When the solution with the NPs is added to one of the reservoirs, the applied electrical field drives particles through the nanopipette, producing a change in the ion current that can be detected. Therefore, to detect NPs and study their different properties, nanopipettes of very small diameters must be produced. The development of nanopipettes began more than a century ago, but even though work has been ongoing to improve the techniques, there is still a long way to go, as seen in [2].

Nowadays, the applications of nanopipettes are diverse, ranging from detection, measurements, and manipulation of biomolecules to imaging of cell surfaces, among others. Due to the applicability of nanopipettes in the field of biomedicine, many research groups keep working to improve the reproducibility in glass nanopipettes fabrication. Glass nanopipettes [3] are not the only type of nanopores used for the detection of NPs, small molecules or cells. The use of biological nanopores [4] and solid-state nanopores [5] has also been reported. The former is currently used to sequence biomolecules such as single-stranded DNA. The latter has similar applicability but the main advantage is that solid-state nanopores are more stable and robust than biological nanopores. Despite most of the literature focuses on solid state nanopores, working with glass nanopipettes has some benefits over other types of nanopores. The fabrication process for nanopipettes is easier and cheaper, they are more easy to manipulate and they are better for using them in combination with an optical tweezer, where the optical trap is formed perpendicular to the nanopipette.

Therefore, in this work we have focused on the fabrication and characterisation of glass nanopipettes for the detection of mesoporous silica NPs, which are commonly used as a drug carrier in treatments. The size of

these NPs was expected to be around 100 nm. Thus, we aimed to find one or several fabrication protocols for the nanopipettes with a diameter at the tip (\mathbf{d}), in principle of about 200 – 300 nm. For this, we used a Laser-Based Micropipette Puller (Sutter Instrument P-2000). Once the nanopipettes were produced, they were filled with a salt solution and we measured their conductance ($G = 1/R$). One of our objectives has been to come up with a formula from which we could be able to extract the diameter of the tip (\mathbf{d}) from the conductance (\mathbf{G}) and avoid going to the scanning electron microscope (SEM), where the value of \mathbf{d} can be measured with exactitude. Finally, to test the functionality of our nanopipettes our last objective has been to perform resistive-pulse sensing experiments with silica NPs using a Coulter counter.

II. EXPERIMENTAL

A. Fabrication of the nanopipettes

The first step in our study has been to fabricate the nanopipettes. To do so, we have used a Laser-Based Micropipette Puller (Sutter Instrument P-2000) (FIG. 1-a) and quartz glass capillaries with inner and outer diameters of 0.2 mm and 0.5 mm, respectively. To produce nanopipettes with different tip sizes and geometries, the P-2000 has five different parameters that we can change: HEAT (\mathbf{H}), FILAMENT (\mathbf{F}), VELOCITY (\mathbf{V}), DELAY (\mathbf{D}) and PULL (\mathbf{P}).

Each of the parameters has a different effect on the geometry of the resulting nanopipette, especially on \mathbf{d} and the taper length (\mathbf{t}). The taper length is the length from where the capillary starts to narrow to its tip, as seen in FIGs. 2-f and 2-g. Here below, as can be consulted in the manual of the puller [6], we briefly describe each of them:

1. \mathbf{H} (range: 0 – 999) specifies the output power of the laser, and consequently, the amount of energy supplied to the glass.
2. \mathbf{F} (r: 0 – 15) specifies the scanning pattern of the laser beam.

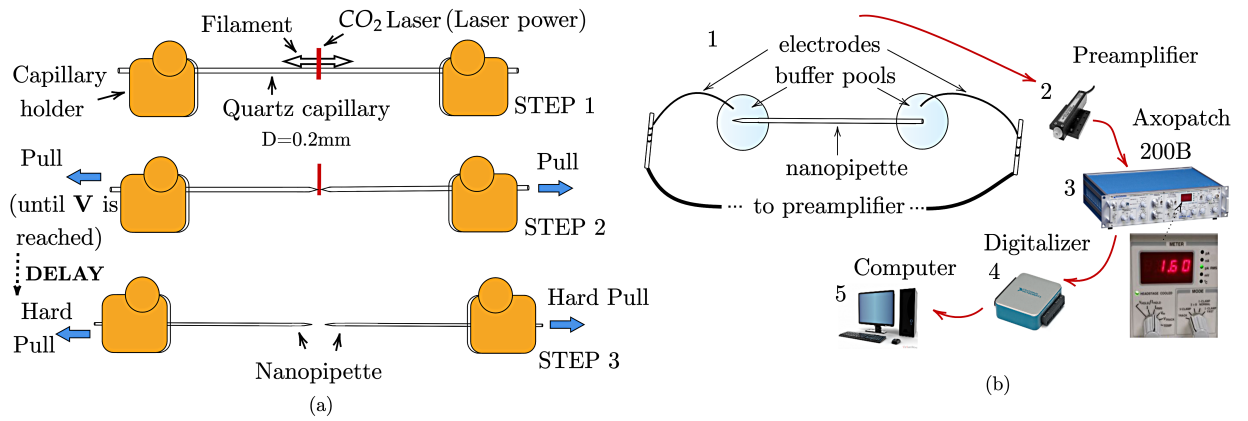


FIG. 1: (a) Fabrication of the nanopipettes using the Laser-Based Micropipette Puller. (b) Steps of the measurement of the electrical conductance of the nanopipette. The electrodes are directly attached to the Axopatch's preamplifier (2). The Axopatch filters the current-time signals before digitalizing them with the Digitalizer (3 and 4). Finally, we monitored and recorded the intensity traces using a LabView application (5).

3. V (r: 0 – 255) specifies the velocity at which the puller bar must be moving before the hard pull is executed. It determines the point at which the HEAT is turned off.
4. D (r: 0 – 255) controls the timing of the start of the hard pull relative to the deactivation of the laser.
5. P (r: 0 – 255) controls the force of the hard pull.

According to [6], a higher value of H , V and P contributes to obtain a higher t and a lower d . In order to obtain pipettes with a given tip size, different protocols were used. A protocol is the set of puller's parameters that we give to obtain a nanopipette in a given range of d .

We start the fabrication of a nanopipette by fixing the quartz capillary in the capillary holder of the pipette puller. A laser with a certain power H is then focused on the capillary and moved parallel to the glass, according to the value of F , heating a larger or smaller area of the capillary. During this process, the capillary is under tension and it ends begin to separate as the glass melts. The more the capillary melts, the faster the ends separated. Finally, when a certain V is reached by the separating ends, the laser is turned off and after the delay time D , a hard pull is exerted on the capillary. The force of the pull is controlled by P .

B. Characterisation of the nanopipettes

1. Optical characterisation

We used an optical microscope to capture the first images of the nanopipettes. As can be seen in FIG. 2-f, these photos were subsequently evaluated with ImageJ which allowed us to measure t for each of them. Nonetheless, the optical microscope lacks the resolution for determining d and the exact geometry near the tip. To accomplish

this, a SEM is necessary.

2. Measurement of the electrical conductance

After the fabrication of the nanopipettes, they were filled with a 10 mM or 100 mM KCl Tris buffer at pH 7.5. Previous to filling them, the pipettes were plasma treated. This process makes their inner surface hydrophilic, which facilitates the filling. To measure G ($G=1/R$) of the filled nanopipette, we used a Axopatch 200B. This is a low noise amplifier which allows us to measure very small currents in the nA range. It basically works as a voltmeter, we apply a voltage difference across the pipette and we measure the resulting current. From the current measurement we can calculate G using Ohm's law. To measure a pipette's G , it is placed between two pools containing a buffer, as shown in FIG. 1-b. Ag/AgCl electrodes are placed inside the pools [7]. This electrodes convert the K^+ and Cl^- ions flowing through the pipette into electrons which are then measured by the Axopatch 200B. To reduce noise during the measurements, the pipette and the preamplifier are placed inside a Faraday cage. We took measurements of the current at various positive and negative voltages to calculate the conductance of the nanopipettes.

3. Scanning electron microscope (SEM)

We had to use the SEM to measure an exact value of d (FIGs. 2-a-e). Before being used in the SEM, the nanopipettes needed to be chopped to a specific size and then sputtered with carbon, coating them with an additional layer (~ 10 nm) of a conductive material and rendering them unusable.

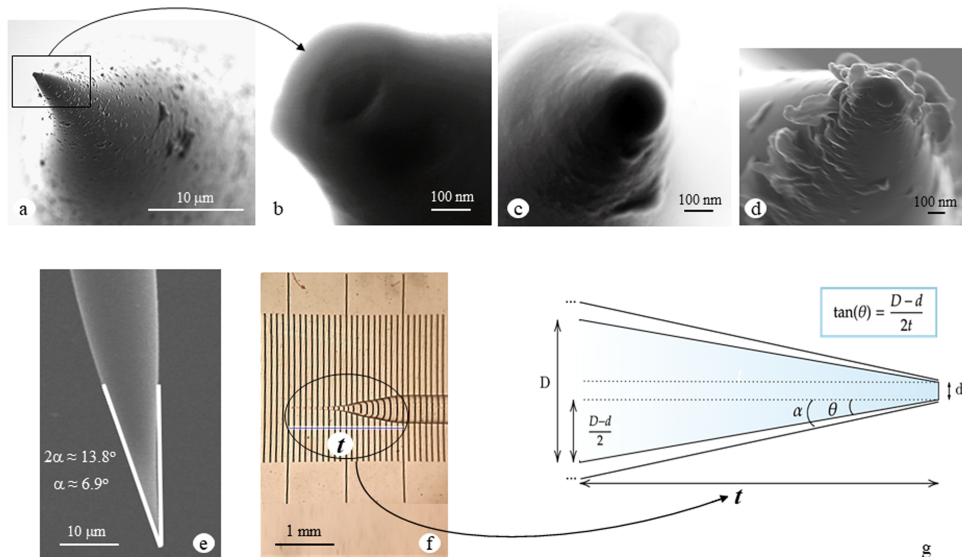


FIG. 2: (a) Zoom out of the tip of a nanopipette with protocol A (SEM image). (b) Protocol A with a tip of 171 nm (SEM image). (c) Protocol A' with a tip of 105 nm (SEM image). (d) Protocol B with a tip of 175 nm (SEM image). (e) Angle α of the tip (SEM image). (f) Optical image with t . (g) Geometric schema of the tip of the nanopipette.

C. Nanoparticles

The NPs were dispersed in a 10 mM KCl solution at pH 11. To make sure that the NPs were dispersed, they were sonicated for about 3 – 4 h. After sonication, we measured their size distribution using a DLS (Dynamic Light Scattering). Finally, to eliminate big aggregates of NPs that were still present in the solution after sonicating, they were filtered with a filter that eliminates particles bigger than 200 nm.

The detection of these NPs by nanopipettes was done with resistive-pulse techniques that are based on the idea of the Coulter counter ([8],[9]). During translocation, NPs partially block the nanopore, resulting in a variation of the current measured by the Axopatch [5].

III. ANALYSIS AND RESULTS

A. Size of the nanopipettes

We were initially interested in creating nanopipettes with a certain d in order to undertake subsequent detection of mesoporous silica NPs. As we have mentioned before, the pulling parameters of the laser puller were found to directly affect the morphology of the glass nanopipettes.

We present the protocols we obtain for producing nanopipettes with 200-300 nm at the tip in TABLE I and II. The protocols contain two lines because each has different functions. In the first line, part of the glass melts and is pulled apart without a hard pull. Then in the second line we start from a thinner capillary, and the hard pull divides it into two nanopipettes.

Furthermore, we made slight variations of each of these protocols to see if the variation of the parameter had a

TABLE I: First protocol

Prot. A	H	F	V	D	P
line 1	450	0	40	255	0
line 2	450	0	45	128	50

TABLE II: Second protocol

Prot. B	H	F	V	D	P
line 1	500	0	20	255	0
line 2	500	0	35	128	80

TABLE III: Tip size

Protocol	A	A'	A''	B	B'
N	14	4	7	3	5
d_{SEM} (nm)	240 ± 20	220 ± 50	250 ± 30	160 ± 40	140 ± 50

influence on the final nanopipette. The variations of the protocols were made maintaining all the parameters except one. Protocol A' and A'' were variations of protocol A changing P of the 2nd line to 47 and V of the 2nd line to 43, respectively. Similarly, protocol B' is a variation of B changing P of the 2nd line to 85. We have computed the mean and deviation of the tip size of each of the protocols from the measures taken with the SEM (d_{SEM}) (FIGs 2 b-d). The results are presented in TABLE III where N is the number of nanopipettes measures from each protocol.

There are several observations we can make from these results. We followed the manual [6] to adjust d , increasing or decreasing its diameter making variations in P and V .

We wanted to see how much different parameters affected the final pipette but we had no feeling how much changing them affected the final pipette because it is not stated in the P-2000 manual. We tried changing them by a few small values but there was almost no difference between the original protocol and the variation.

Finally, there are other factors which are difficult to control and can also affect the geometry and tip size of

the nanopipette.

B. Conductance and tip size of the nanopipette

The measurements we have made using the Axopatch, for 10 mM, gives us values of \mathbf{G} and \mathbf{R} in the order of 5 – 7 nS and 150 – 200 M Ω respectively. In order to be able to estimate \mathbf{d} , we needed to find a formula that would relate \mathbf{G} to \mathbf{d} . In this sense, we can think of the nanopipette as a wire, the resistance of which depends on its geometry ($R = \frac{\rho L}{A}$, $G = \frac{gA}{L}$). Thus, the conductance of the nanopipette has been calculated taking into account that its geometry can be approximated to a cone. Therefore we obtain (1), where g is the conductivity of the solution ($g = 1.28$ S/m for 100 mM and $g = 0.21$ S/m for 10 mM) and \mathbf{d} , \mathbf{t} , \mathbf{D} can be seen in FIG. 2-g:

$$G_{cone} = g \left(\frac{\pi d D}{4t} \right) \quad (1)$$

Additionally, as other articles such as [5] mention, a term of access conductance can be added to the total conductance of the nanopipette. Kowalczyk et al. states that the electrical resistance between two spherical electrodes in a medium does not depend on the distance between the two electrodes but on their sizes [5]. In our case, we need to add this contribution ($R_{access} = g/2d$) in series to the total resistance. Thus, the final resistance is $R = R_{cone} + R_{access}$. Taking the approximation $\tan(\theta) = \frac{D-d}{2t} \approx \frac{D}{2t}$ (because $d \ll D$), where θ is the inner half angle of the aperture as can be seen in FIG.2-g, the conductance can be expressed as:

$$G = \frac{1}{R_{cone} + R_{access}} = g \left(\frac{2\pi d D}{8t + \pi D} \right) = g \left(\frac{2\pi d \tan(\theta)}{4 + \pi \tan(\theta)} \right) \quad (2)$$

We have divided G by g in (3) because the conductivity has a dependence on the salt concentration and thus the ratio G/g is independent of the concentration. This is significant because we initially used a buffer with 100 mM KCl, but after observing in the SEM that this concentration formed salt crystallization at the tip, we decided to change it to 10 mM KCl.

$$\frac{G}{g} = \frac{2\pi d \tan(\theta)}{4 + \pi \tan(\theta)} = md \quad \left(m = \frac{2\pi \tan(\theta)}{4 + \pi \tan(\theta)} \right) \quad (3)$$

Initially, using equation (2), we wanted to estimate \mathbf{d} from \mathbf{G} taking \mathbf{t} as a mean of the taper length we measured in the images of the optical microscope. Using the optical microscope is faster and less costly than using the SEM and \mathbf{t} was the only data we could extract from the optical images. From the cone with $t_{mean} = 1.8$ mm and $\mathbf{D} = 0.2$ mm (FIG 2-g), the associated angle is $\theta \approx 3.2^\circ$. If we were to use this angle θ to calculate \mathbf{d} from \mathbf{G} , we would get the values given in the line $\theta = 3.2^\circ$ in FIG. 3-a. However, in this figure, the line $\theta = 3.2^\circ$ did not agree with the data taken with 100 mM KCl and 10 mM KCl.

Therefore, we did a linear fit of the data in FIG. 3-a from which we could calculate, using (3) and the slope

of the fit (m), an angle $\theta = 4.8^\circ$. This value makes sense and agrees with the SEM images (FIG 2-g) where we measured an average angle of $\alpha = 6.9^\circ$ (outer angle of the cone). Indeed, it makes sense that this angle α is somewhat larger than $\theta = 4.8^\circ$, obtained with the adjustment, because α is the exterior angle while θ is the interior angle.

To conclude, the macroscopic measurement corresponding to \mathbf{t} is not useful to make good estimates of \mathbf{d} from \mathbf{G} because $t = 1.8$ mm approximates a certain cone that does not resemble the geometrical shape of the pipette. Therefore, as the part of the pipette that contributes most to the calculation of the resistance is the narrowest part, it is in our interest to measure this area well. This is done by extracting from the fit an angle $\theta = 4.8^\circ$ which agrees with the SEM images in FIG. 2-e.

C. Translocation of NPs

In FIG. 3-b we can see the size distributions we have measured with the DLS. We observed that using a filter of 200 nm, we could get rid off the aggregates that are visible in the blue tail in FIG. 3-b. This is important as big aggregates could block the nanopipette during the experiments. We see that for the filtered NPs we have a mean size of about 100 nm. So they should translocate through a 200 – 300 nm nanopipette.

For the experiments, the NPs are placed in the pool where we have the nanopipette tip. Applying a negative voltage, we have observed translocation of NPs as we can see in FIG. 3-c and FIG. 3-d. We see peaks of different magnitudes. According to [10], this ratio is proportional to the particle size. This is consistent with the fact that we have a large dispersion of particle sizes as can be seen in FIG. 3-b. On the other hand, the shape of the translocation, as shown in FIG. 3-d, is consistent with the passage of a sphere through a cone. Thus, the point where the particle passes through the narrowest place of the pipette is related to the maximum current drop.

IV. CONCLUSIONS

We have been able to produce, using two different protocols and their variations, nanopipettes with \mathbf{d} of 200–300 nm. Additionally, we have measured their \mathbf{G} using a Coulter counter method and found a formula, according to their geometry (angle α or θ), to estimate \mathbf{d} . We have determined that $\theta = 4.8^\circ$ is the parameter value that allows us to make a better estimation of \mathbf{d} from \mathbf{G} and it is the one we will use from now on. Moreover, we have dispersed mesoporous silica NPs using DLS in a pH 11 using a filter of 200 nm to eliminate aggregates and we have determined the size of the NPs around 100 nm. Finally, we have tested the functionality of our nanopipettes by making tests in translocation experiments, which have given satisfactory results.

The most significant outcome of our work is that the

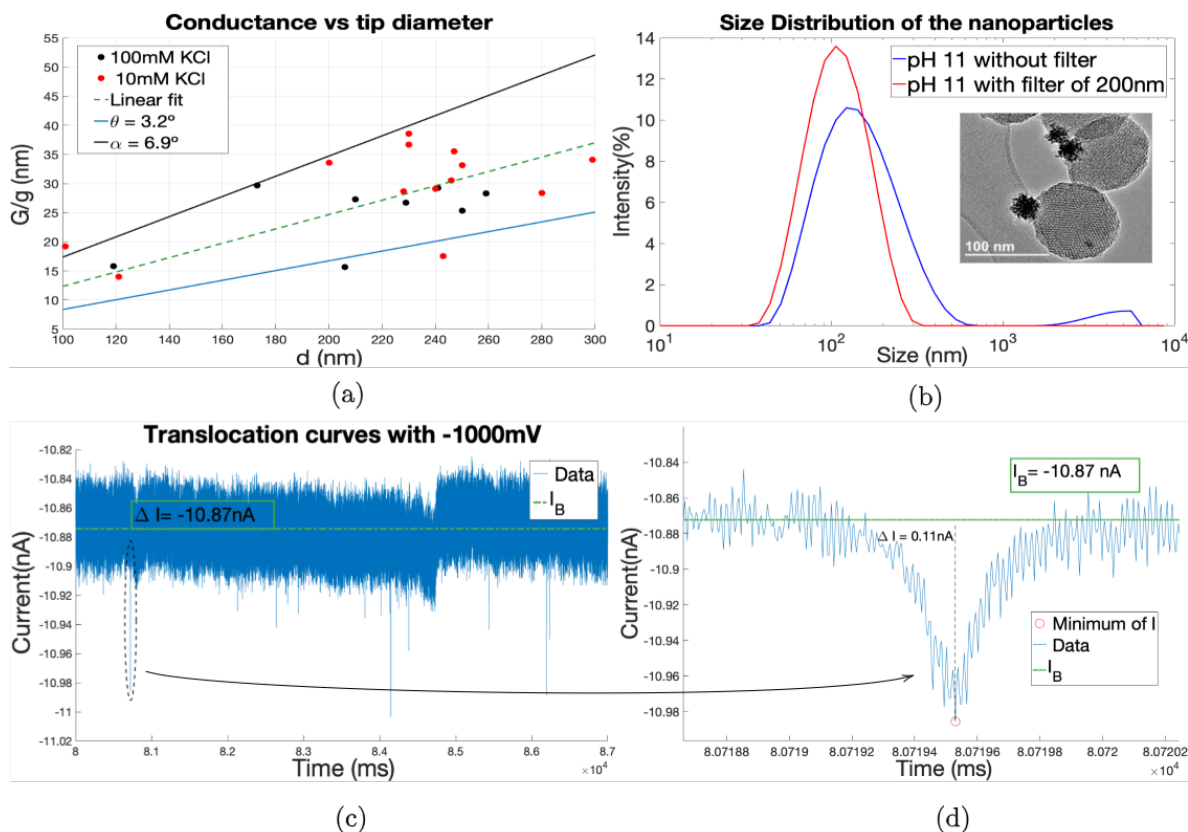


FIG. 3: (a) Experimental data of conductance/conductivity where I_B is the baseline current. (b) Measures of the size distribution of mesoporous silica NPs using DLS. (c) Translocations of NPs for -1000 mV. (d) Zoom of a current blockage in (c).

pipettes we have produced, in the range of 200 – 300 nm, can be used in future work to study mesoporous silica NPs because the experiments carried out with them have been satisfactory. It would also be interesting to study the useful lifetime of nanopipettes after being used to understand when a nanopore becomes unusable. To do so, we could take several measurements of the conductance in order to observe changes or not in it. This could be explained by the obstruction of the channel due to the accumulation of deposits inside the nanopipette undetectable by SEM. Eventually, it would be practical

to work with a greater sample (N) in order to obtain less deviation in our calculations and validate our results.

Acknowledgments

I would like to thank my advisor, Alejandro Colchero, for his guidance and patience as well as everyone in the Small Biosystems Lab and especially Felix Ritort for the opportunity to carry out the experiments in his Lab.

- [1] Hurley, J. "Sizing particles with a Coulter counter." *Biophysical Journal*, **10**(1), 74–79 (1970).
- [2] Stanley, J. and Pourmand, N. "Nanopipettes - The past and the present." *APL Mater.* **8**, 100902 (2020).
- [3] Karhanek, M. et al. "Single DNA Molecule Detection Using Nanopipettes and Nanoparticles Nano Letters" **5**(2), 403-407 (2005).
- [4] Ying, Y.L.; Cao, C.; Long, Y.T. "Single molecule analysis by biological nanopore sensors". *The Analyst*, **139**(16), 3826–(2014).
- [5] Kowalczyk, S.W. et al. "Modeling the conductance and DNA blockage of solid-state nanopores." *Nanotechnology*, **22**(31), 315101–(2011).
- [6] Sutter Instrument Company. *Sutter Instrument P-2000 Operation Manual* (2020).
- [7] Wei, C.; Bard, A.J.; Feldberg, S.W. "Current Rectification at Quartz Nanopipet Electrodes." *Analytical Chemistry*, **69**(22), 4627–4633 (1997).
- [8] Yang, L.; Yamamoto, T. "Quantification of Virus Particles Using Nanopore-Based Resistive-Pulse Sensing Techniques." *Frontiers in Microbiology*, **7**, 1500–(2016).
- [9] Wang, Z. et al. "Nanopipette: a potential tool for DNA detection." *The Analyst*. **144** (2019).
- [10] Yi, W. et al. "Glass nanopipette sensing of single entities" *Journal of Electroanalytical Chemistry (IF4.464)* – (2022).